Global and Planetary Change 112 (2014) 64–78

Contents lists available at ScienceDirect

Global and Planetary Change

journal homepage: www.elsevier.com/locate/gloplacha

Are there interactive effects of physiological and radiative forcing produced by increased CO_2 concentration on changes of land hydrological cycle?

Jing Peng [a], Li Dan [a,*], Wenjie Dong [a,b]

[a] START Temperate East Asia Regional Center and Key Laboratory of Regional Climate-Environment for Temperate East Asia, Institute of Atmospheric Physics, Chinese Academy of Sciences, Beijing 100029, China
[b] State Key Laboratory of Earth Surface Processes and Resource Ecology, Beijing Normal University, Beijing 100875, China

ARTICLE INFO

Article history:
Received 16 January 2013
Received in revised form 13 November 2013
Accepted 25 November 2013
Available online 1 December 2013

Keywords:
interactive effect
CO_2-physiological forcing
CO_2-radiative forcing
precipitation
transpiration
runoff
CMIP5

ABSTRACT

Three coupled climate–carbon cycle models including CESM (Community Earth System Model), CanEsm (the Canadian Centre for Climate Modelling and Analysis Earth System Model) and BCC (Beijing Climate Center Climate System Model) were used to estimate whether changes in land hydrological cycle responded to the interactive effects of CO_2-physiological forcing and CO_2-radiative forcing. No signs could be indicated that the interactive effects of CO_2-physiological forcing and CO_2-radiative forcing on the hydrological variables (e.g. precipitation, evapotranspiration and runoff) were detected at global and regional scales. For each model, increases in precipitation, evapotranspiration and runoff (e.g. 0.37, 0.18 and 0.25 mm/year^2) were simulated in response to CO_2-radiative forcing (experiment M3). Decreases in precipitation and evapotranspiration (about −0.02 and −0.09 mm/year^2) were captured if the CO_2 physiological effect was only accounted for (experiment M2). In this experiment, a reverse sign in runoff (the increase of 0.08 mm/year^2) in contrast to M3 is presented. All models simulated the same signs across Eastern Asia in response to the CO_2 physiological forcing and radiative forcing: increases in precipitation and evapotranspiration only considering greenhouse effect; reductions in precipitation and evapotranspiration in response to CO_2-physiological effect; and enhanced trends in runoff from all experiments. However, there was still a large uncertainty on the magnitude of the effect of transpiration on runoff (decreased transpiration accounting for 8% to 250% of the increased runoff) from the three models. Two models (CanEsm and BCC) attributed most of the increase in runoff to the decrease in transpiration if the CO_2-physiological effect was only accounted for, whereas CESM exhibited that the decrease in transpiration could not totally explain the increase in runoff. The attribution of the CO_2-physiological forcing to changes in stomatal conductance versus changes in vegetation structure (e.g. increased Leaf Area Index) is an issue to discuss, and among the three models, no agreement appeared.

1. Introduction

There exist two ways of effect of the increasing CO_2 concentration in the atmosphere on climate change and hydrological cycle via its greenhouse radiative effect and the effect on plant physiology as reported by the previous studies (Cramer et al., 2001; Gerten et al., 2007; Boucher et al., 2009; Cao et al., 2009; Bala et al., 2010; Cao et al., 2010).. The CO_2-physiological forcing influences the biophysical characteristics (such as stomatal resistance and albedo) and leaf area index (LAI) to alter the energy and water flux between the biosphere and the atmosphere, via the biophysical and biogeochemical pathways (Piao et al., 2007; Bala et al., 2011). For example, the elevated CO_2 concentration in the atmosphere is expected to reduce canopy conductance and thus leads to reduction in canopy transpiration (Field et al., 1995; Cao et al., 2009; Barton et al., 2012). This change could induce the decrease in evapotranspiration (the sum of canopy evaporation, canopy transpiration, and soil evaporation), prompting changes in clouds, and involving changes in land surface energy budget and surface temperature, thus constructing changes in the atmospheric water vapour and water cycle (Boucher et al., 2009; Cao et al., 2010; Andrews et al., 2011).

Some studies have used the experiments produced by models to investigate the possible response of regional and global hydrological cycle to physiological and radiative forcing by elevated CO_2 levels in the atmosphere. All of the experiments among various models demonstrate a significant increase in temperature (Doutriaux-Boucher et al., 2009), a significant increase in precipitation (Risnen, 2002; Sugi and Yoshimura, 2004), an increase in evapotranspiration (Boucher et al., 2009; Cao et al., 2010; Andrews et al., 2011), and an increase in runoff (Betts et al., 2007) at global or regional scales in response to CO_2-radiative forcing. There is no guarantee of consistencies in the trends of all the hydrological variables including precipitation, evapotranspiration and runoff

* Corresponding author.
E-mail address: danli@tea.ac.cn (L. Dan).

0921-8181
http://dx.doi.org/10.1016/j.gloplacha.2013.11.007

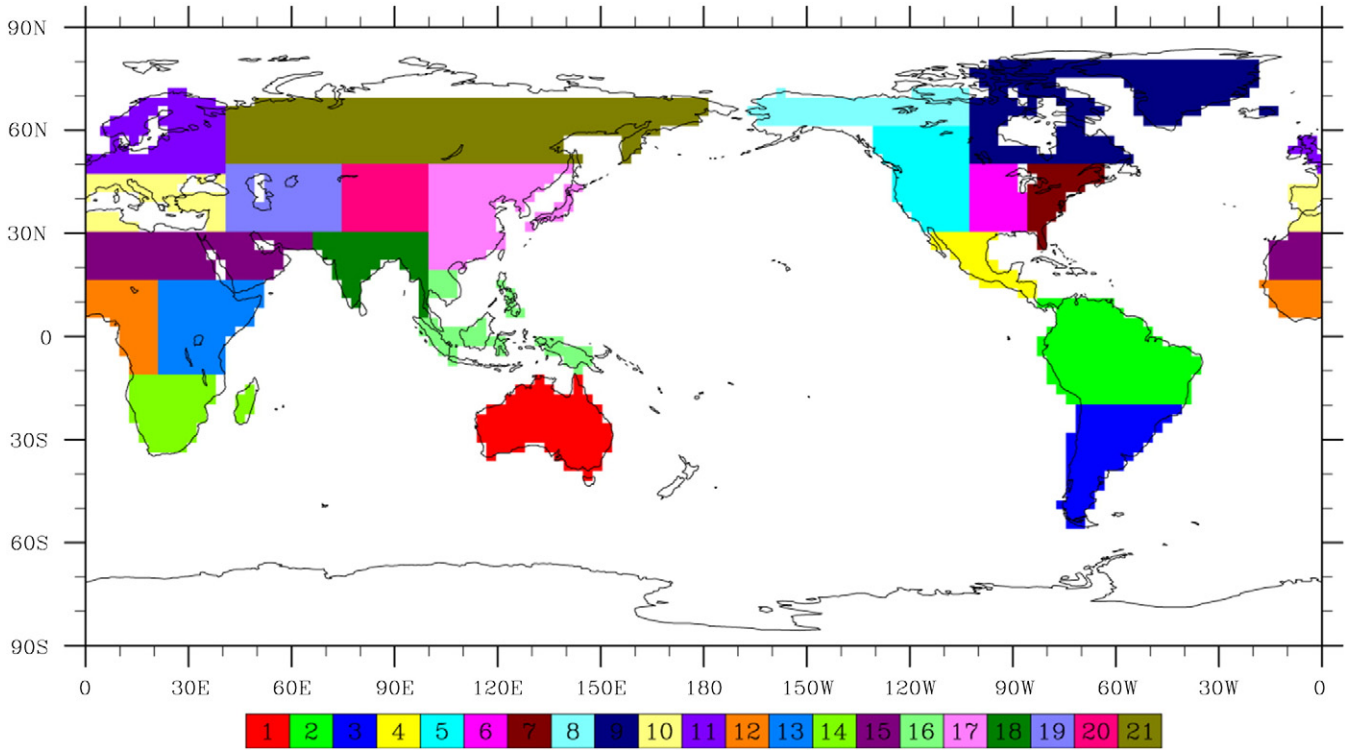

Fig. 1. Map of regions used in the analysis as defined by Giorgi and Francisco (2000).

Table 1
Percentages of the areas over the 21 regions and world, where differences between the results of M1 and M2 + M3 are not statistically significant at the 5% level using the student *t*-test. Units are %.

ID	Region	Precipitation			Evapotranspiration			Runoff			Transpiration		
		CESM	CanEsm	BCC	CESM	CanEsm	BCC	CESM	CanEsm	BCC	CESM	CanEsm	BCC
1	Australia	100	100	100	100	100	100	100	100	100	100	100	100
2	Amazon Basin	100	100	100	100	100	100	100	100	100	100	100	100
3	Southern South America	100	100	100	100	100	100	100	100	100	100	100	100
4	Central America	100	100	100	100	100	100	100	100	100	100	100	100
5	Western North America	100	100	100	100	100	100	100	100	100	100	100	100
6	Central North America	100	100	100	100	100	100	100	100	100	100	100	100
7	Eastern North America	100	100	100	100	100	100	100	100	100	100	100	100
8	Alaska	100	100	100	100	100	100	100	100	100	100	100	100
9	Greenland	100	100	100	100	100	100	100	100	100	100	100	100
10	Mediterranean Basin	100	100	100	100	100	100	100	100	100	100	100	100
11	Northern Europe	100	100	100	100	100	100	100	100	100	100	100	100
12	Western Africa	100	100	100	100	100	100	100	100	100	100	100	100
13	Eastern Africa	100	100	100	100	100	100	100	100	100	100	100	100
14	Southern Africa	100	100	100	100	100	100	100	100	100	100	100	100
15	Sahara	100	100	100	100	100	100	100	100	100	100	100	100
16	Southeast Asia	100	100	100	100	100	100	100	100	100	100	100	100
17	East Asia	100	100	100	100	100	100	100	100	100	100	100	100
18	South Asia	100	100	100	100	100	100	100	100	100	100	100	100
19	Central Asia	100	100	100	100	100	100	100	100	100	100	100	100
20	Tibet	100	100	100	100	100	100	100	100	100	100	100	100
21	North Asia	100	100	100	100	100	100	100	100	100	100	100	100
22	World	100	100	100	100	100	100	100	100	100	100	100	100

among different models, responding to CO_2-physiological forcing, when biophysical processes have been coupled to the climate system models (Kergoat et al., 2002; Gedney et al., 2006; Betts et al., 2007; Gerten et al., 2007; Piao et al., 2007; Boucher et al., 2009). Given this premise, one of the most uncertainties simulated by all of the models is the sign of runoff changes in response to the CO_2-physiological forcing (Gedney et al., 2006; Betts et al., 2007; Piao et al., 2007). This could be contributed to the large uncertainty behind precipitation and evapotranspiration, because runoff is generally represented by the difference between the quantities (precipitation and evapotranspiration) (Piao et al., 2007). When CO_2-physiological forcing is only considered, dissimilar simulated results for the magnitude and the sign of changes in precipitation and runoff over the land have been revealed in the previous studies (Gedney et al., 2006; Piao et al., 2007). For example, associated with the CO_2 physiological effect, a slightly greater precipitation change had been simulated by HadSM3 (the mixed-layer ocean version of HadCM3) (Betts et al., 2007). However, a diverse result was suggested by Andrews et al. (2011) using the Met Office Hadley Centre HadCM3LC over land regions (Andrews et al., 2011) in contrast to Betts's conclusion.

The aspect of combined effect of CO_2-physiological forcing and CO_2-radiative forcing is usually inspected using coupled climate carbon cycle models under the elevated CO_2 concentration in the atmosphere (Doutriaux-Boucher et al., 2009; Andrews et al., 2011). There is similar deficiency among all of the experiments that none of the models considered the effect caused by interaction of the two different forcing. Changes in hydrological processes in response to interaction between the CO_2-physiological forcing and CO_2-radiative forcing were neglected in these studies (Piao et al., 2007; Boucher et al., 2009; Cao et al., 2010). For instance, Cao et al. (2010) investigated the response of climate change to the CO_2-physiological forcing, arising from the difference between the combined effect of the CO_2-physiological and CO_2-radiative forcing and the effect of CO_2-radiative forcing. All of the simulated results have not taken into account whether or not the interactive effects of CO_2 physiological and radiative forcing via the feedback of the interaction between them could influence the surface characteristics such as albedo and roughness, alter surface energy balance, and even affect water flux at global and regional scales.

It is well known that the CO_2 concentration rise in the atmosphere is one of key factors controlling the climate change and hydrology cycle (Solomon et al., 2009; Tenhunen et al., 2009; Gillett et al., 2011; Zhu et al., 2012). However, whether or not the interactive effects of CO_2 physiological and radiative forcing on the magnitude and sign of hydrological variables of precipitation, evapotranspiration and runoff at global and regional scales have not been taken into account in the previous studies. In this analysis, we examined whether or not the interactive effects on the hydrological cycle could be captured, how the responses of the hydrological variables to the CO_2-physiological forcing and CO_2-radiative forcing are presented by the three fully coupled climate and carbon models including CESM, CanEsm and BCC during the 140 years over the world and 21 regions (Fig. 1) that have been detailed by Peng et al. (2012).

2. Data and method

In this analysis, we have used 3 models from phase 5 of the Coupled Model Intercomparison Project (CMIP5) including CESM (first-generation Community Earth System Model), CanEsm (second-generation the Canadian Centre for Climate Modelling and Analysis Earth System Model) and BCC (first-generation Beijing Climate Center Climate System Model). CESM is a fully coupled climate model for simulating the earth's climate system produced by the National Center for Atmospheric Research (NCAR) (http://www.cesm.ucar.edu/models/cesm1.0/). It consists of four separate models simultaneously simulating the earth's atmosphere, ocean, land surface and sea-ice, and one central coupler component. The land component, the Community Land Model version 4.0 (CLM4), has been coupled into CESM. At global and site scales, previous studies had evaluated the simulated results of CLM4 (Bonan et al., 2012). It considered vegetation as plant functional types (PFTs) including 8 tree, 3 shrub, 3 grass, and 2 crop types (Bonan and Levis, 2010). For each PFT, variables (e.g. temperature and humidity) are separately computed for canopy, near-surface, and the leaf surface (Lawrence et al., 2012). At the same time, the mechanism of PFTs competition has also been introduced, such as PFT competition for soil water within each grid cell (Lawrence et al., 2011). In CanESM2, using the Canadian TEM (CTEM) is to model terrestrial ecosystem processes. There are five carbon pools in CTEM including 3 live vegetation pools (leaves, stem and root) and 2 dead carbon pools (litter and soil organic carbon) described by Christian et al., 2010). Based on vapour pressure deficit, a single-leaf photosynthesis approach is used (Leuning, 1995), and stomatal conductance and photosynthesis are calculated via a coupled leaf-level model, with leaf area index estimated from a percentage of the whole-plant carbon balance Christian et al. (2010). BCC is also a fully-coupled carbon and climate model produced by the Beijing Climate Center (Zhang et al., 2011). For the land surface processes, BCC_AVIM has been tested through offline, atmosphere-land coupled as well as fully coupled model via coupler (http://bcc.cma.gov.cn/bcccsm/htm/). It is developed based on the biogeophysical frame of NCAR/CLM3 and incorporates a dynamic vegetation growth model (Ji, 1995; Dan et al., 2005) to describe the seasonal and interannual variation of canopy growth. It also consists of a sub-model for the microbial decomposition of soil organic matter to account for the heterorespiration of soil, one aspect of land carbon cycling, to meet the requirements for participating in the CMIP5. The horizontal resolution of BCC and CanEsm is 2.185° latitude by 2.185° longitude, while the resolution of CESM is 0.9° latitude by 1.25° longitude.

Three experiments of CMIP 5 as described by Peng et al. (2013) are chosen: the combined effect of CO_2-physiological forcing and CO_2-radiative forcing on the hydrological cycle (experiment M1); the contribution of CO_2-physiological forcing neglecting the CO_2-radiative forcing contribution (experiment M2); and the response of the hydrology cycle to the CO_2-radiative forcing with the exception of the CO_2-physiological forcing (experiment M3). With the coupled carbon/climate models, the chosen CMIP5 experiments have been prescribed by 1% increase of CO_2 concentration per year in atmosphere during the period of 1850–1989 (http://cmip-pcmdi.llnl.gov/cmip5/docs/Taylor_CMIP5_ design.pdf). In this study, the focus is to investigate hydrological response to changes in plant physiology e.g. reduced opening of stomata and Earth's global temperature changes over a multi-year timescale associated with CO_2 increasing. The calculations of plant physiology in effect of CO_2-physiological forcing used a 1%/year CO_2 increase from pre-industrial CO_2 concentration to quadrupling. In this experiment M2, the radiation code was fixed the time-invariant CO_2 concentration by 275 ppm. There is little climate change, whereas the concentration of CO_2 input to terrestrial ecosystem increases 1% per year and the changes in biophysical and biogeochemical properties of the vegetation respond to the increase in CO_2 concentration (Taylor et al., 2012). Inversely, in M3, the effect of CO_2-radiative forcing was forced by 1% per year CO_2 increase to quadrupling in radiation package, but the calculations of plant physiology used a fixed pre-industrial CO_2 concentration in vegetation module. Specifically, the radiation code was used rising atmospheric CO_2 concentration with 1% per year (Taylor et al., 2012). Forced in this way, it can be regarded that the terrestrial water cycle only responds to climate change alone. The combined effect of CO_2 radiative and physiological forcing was represented by calculating both plant physiological and radiative transfer using a CO_2 concentration of atmospheric 1%/year CO_2 increase from 275 ppm to quadrupling in radiation package and vegetation module.

In this analysis, interactive effects of CO_2-physiological forcing and CO_2-radiative forcing can be estimated as Eq. (1):

$$\Delta X = Y - (X_1 + X_2) + \varepsilon \quad (1)$$

where ΔX represents the response of the hydrological variable (e.g. precipitation) to the interactive effects of CO_2-physiological forcing and CO_2-radiative forcing; Y is the response of this variable to the combined effect of CO_2-physiological forcing and CO_2-radiative forcing; X_1 represents the response of the identical variable to the effect of CO_2-physiological forcing; X_2 represents its response to the CO_2-radiative forcing.

Fig. 2. Distribution of precipitation trends simulated by CESM, CanEsm and BCC in response to combined CO_2-radiative and physiological forcing (experiment M1) ((a)–(c)), CO_2-physiological forcing (experiment M2) ((d)–(f)), CO_2-radiative forcing (experiment M3)((g)–(i)). Hatched areas are regions where changes are statistically significant at the 5% level using the student *t*-test, units: mm/year^2.

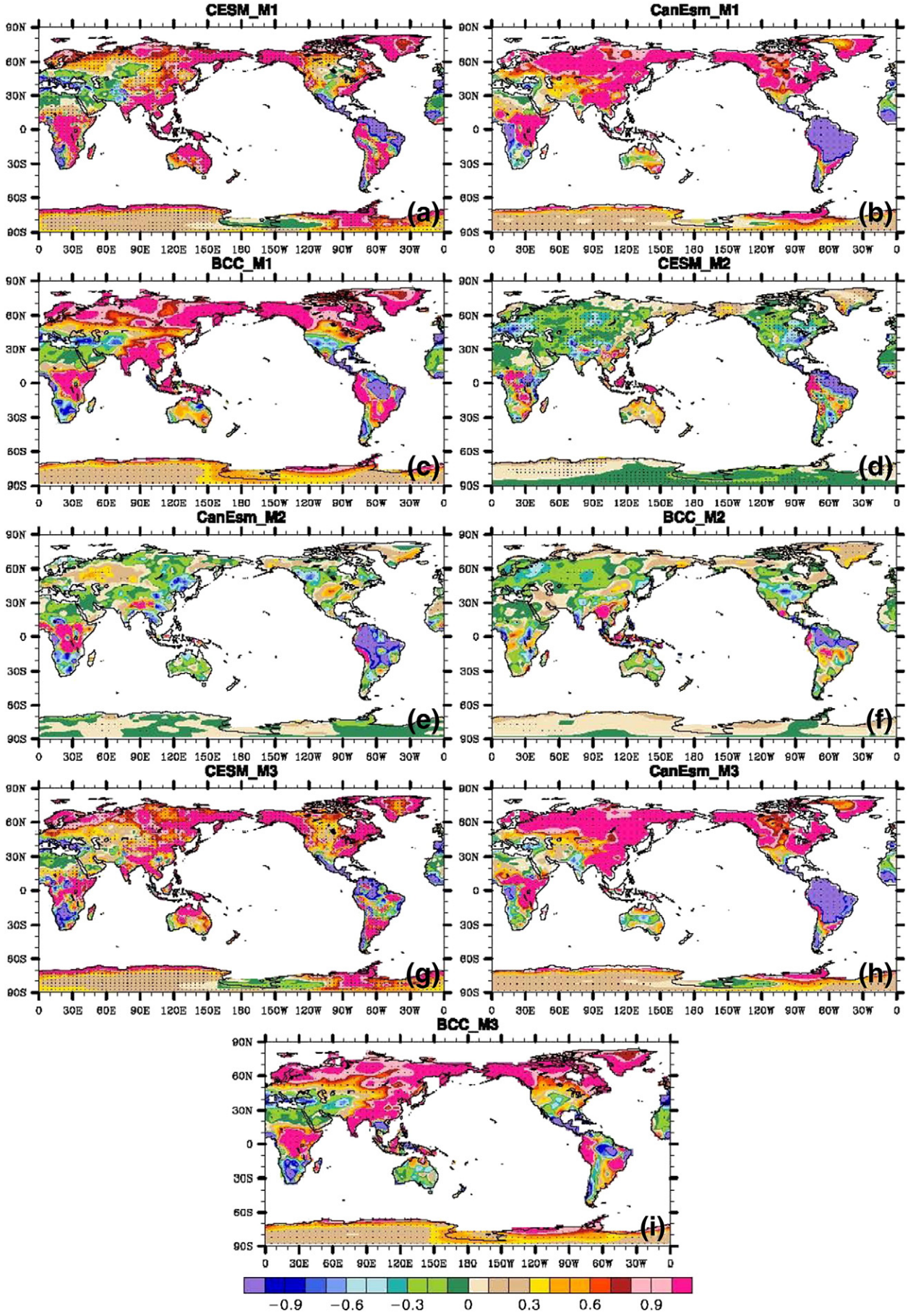
CESM_M1
CanEsm_M1
BCC_M1
CESM_M2
CanEsm_M2
BCC_M2
CESM_M3
CanEsm_M3
BCC_M3
(a)
(b)
(c)
(d)
(e)
(f)
(g)
(h)
(i)
90N
60N
30N
0
30S
60S
90S
0 30E 60E 90E 120E 150E 180 150W 120W 90W 60W 30W 0
−0.9 −0.6 −0.3 0 0.3 0.6 0.9

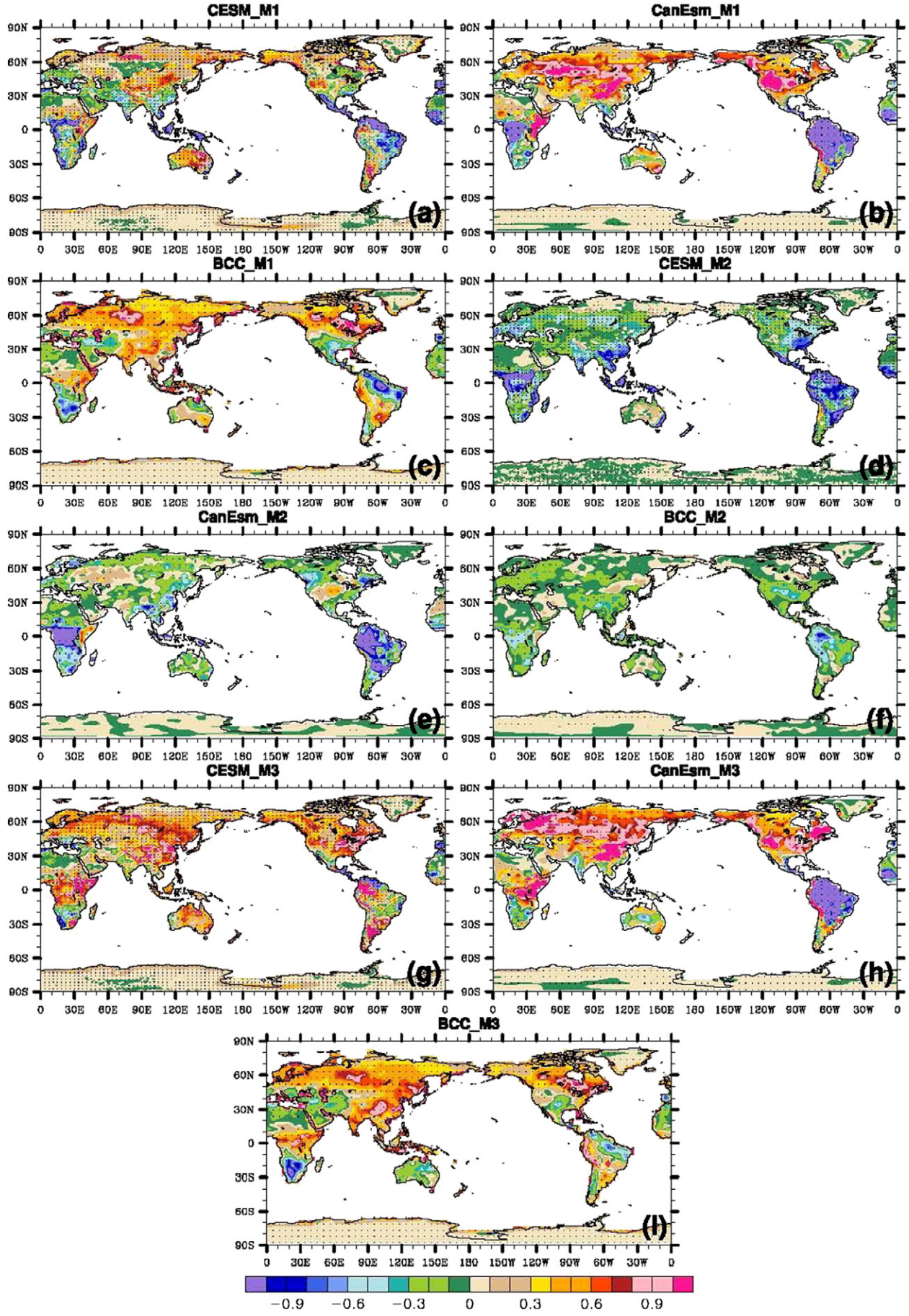

Fig. 3. Same as Fig. 2, but for evapotranspiration trends.

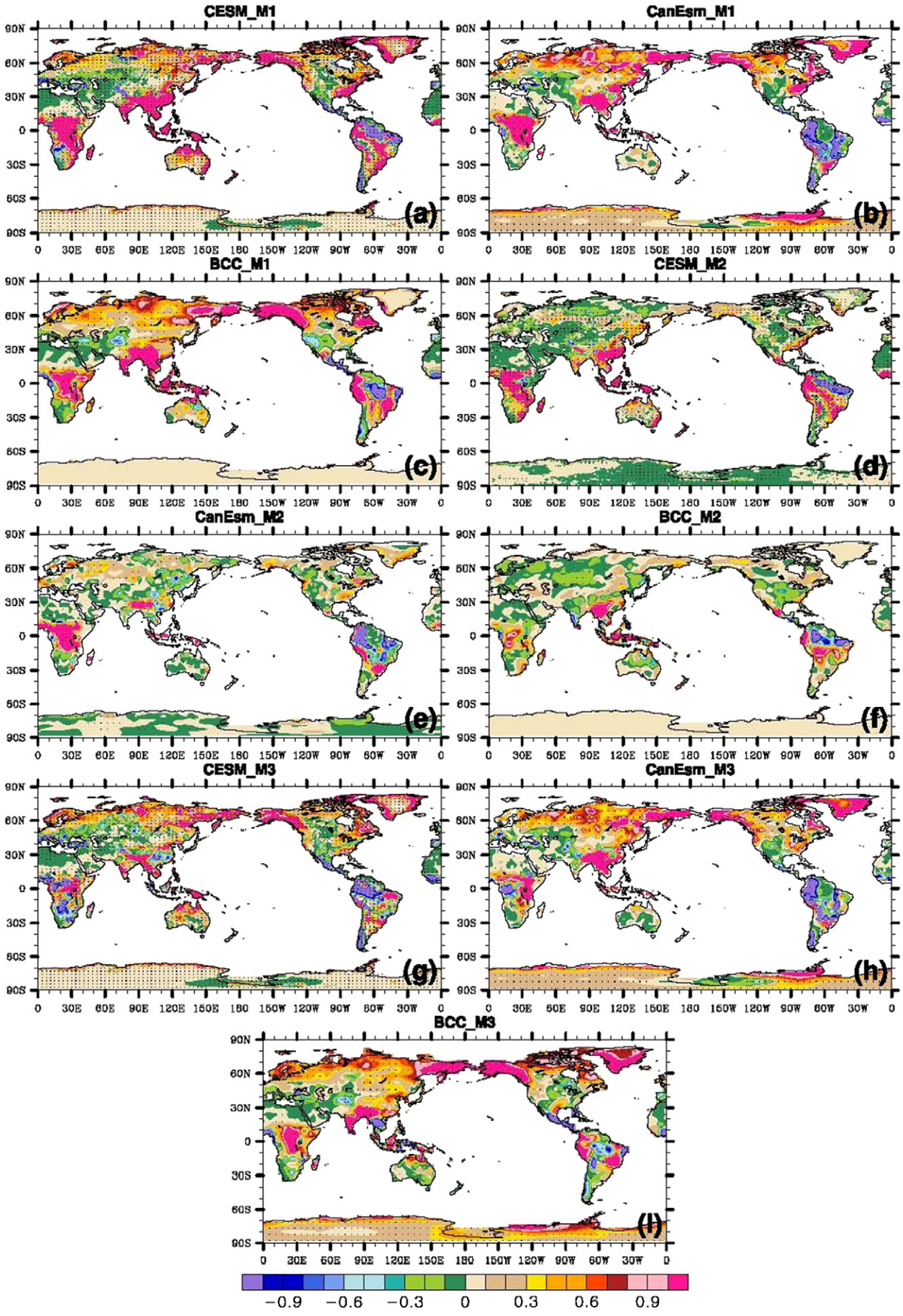

Fig. 4. Same as Fig. 2, but for runoff trends.

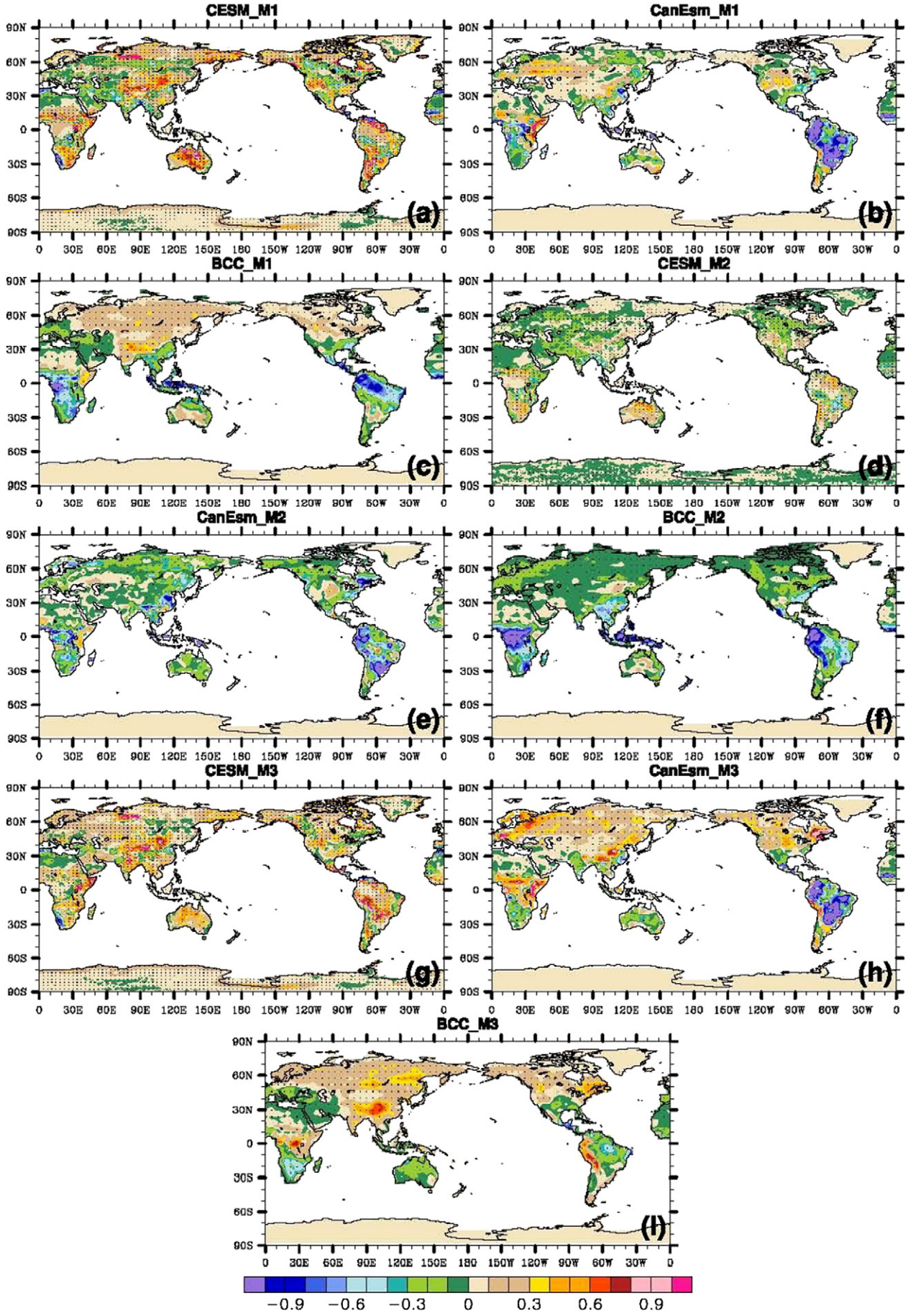

Fig. 5. Same as Fig. 2, but for transpiration trends.

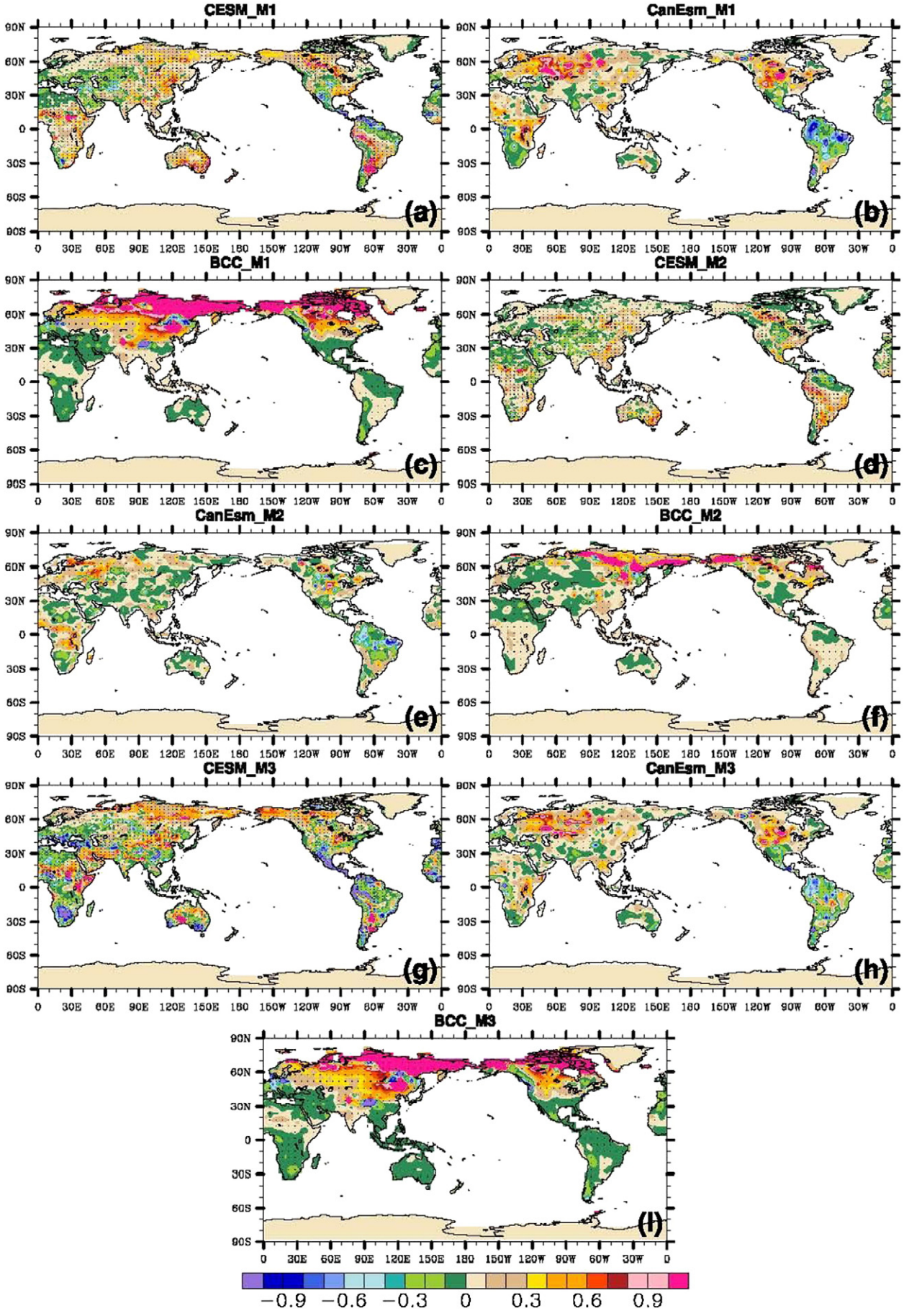

Fig. 6. Same as Fig. 2, but for soil moisture trends, units: kg/m^2/year.

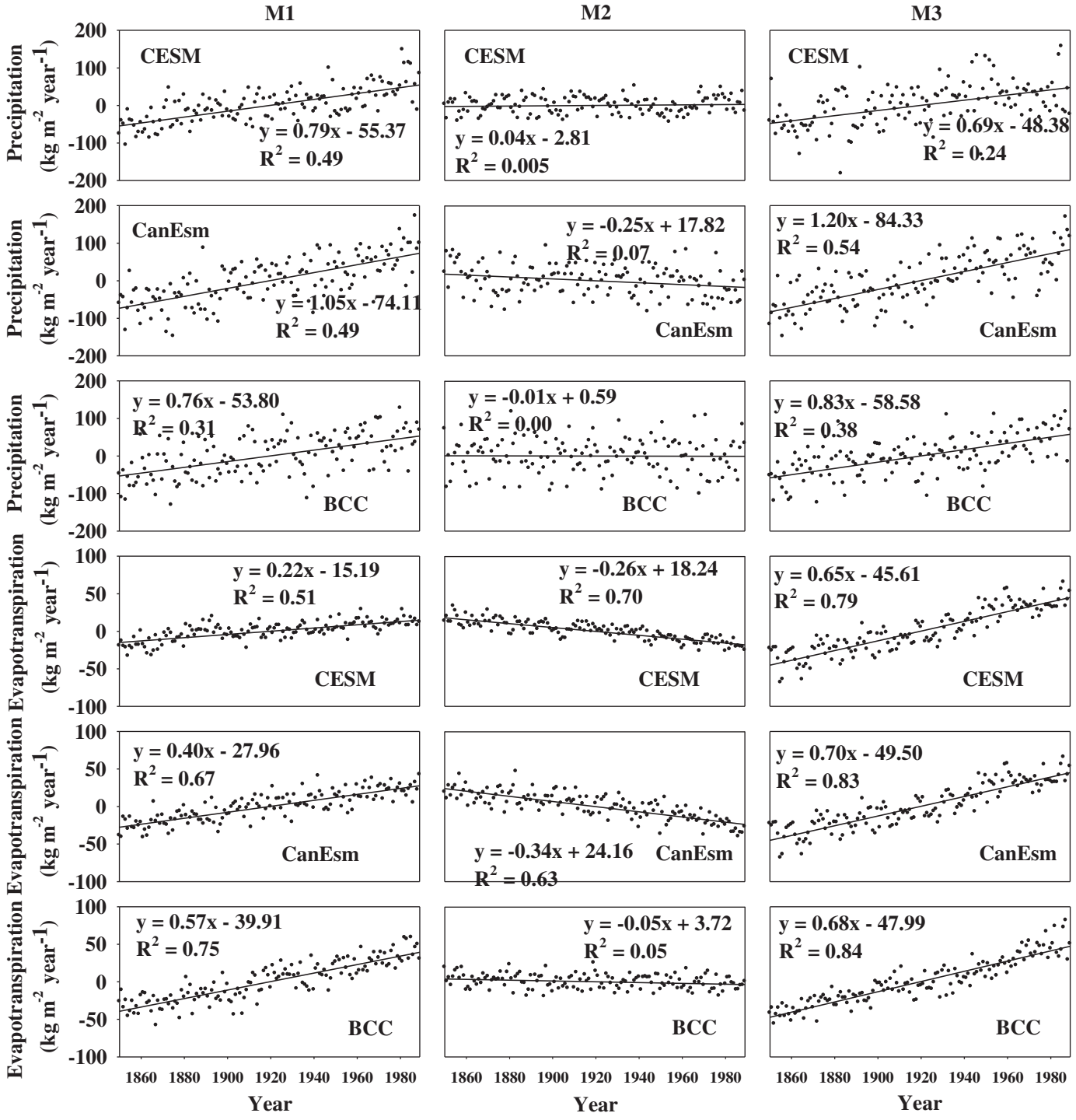

Fig. 7. Simulated annual changes in precipitation and evapotranspiration for the 140 years of the simulations of combined CO_2 physiological and radiative forcing (M1), physiological forcing (M2) and radiative forcing (M3). Lines are regressions and the symbols are averaged values of the Eastern Asia.

3. Results

In Table 1, the proportion of the grids of 21 regions and world is shown and the key hydrological variables (e.g. precipitation, evapotranspiration, runoff and transpiration) have not been significantly influenced by the interactive effects of CO_2-physiological forcing and CO_2-radiative forcing at 5% level using student *t*-test. An inclusion can be drawn that the CO_2-physiological and CO_2-radiative interactive effects on land water cycle are not explicit at global and regional scales.

The response of trends of precipitation, evapotranspiration, runoff, transpiration and soil moisture to a 1%/year increase of atmospheric CO_2 associated with all of the physiological forcing, the radiative forcing, and the combined radiative and physiological forcing is shown in Figs. 2–8. The temperature trend is much higher in response to CO_2-radiative forcing than to CO_2-physiological forcing (2.8 °C/100 year vs. 0.2 °C/100 year across the world and 2.9 °C/100 year vs. 0.4 °C/100 year in Eastern Asia) during the 140 years from CESM, CanEsm and BCC. The simulated land temperature trend in response to CO_2-

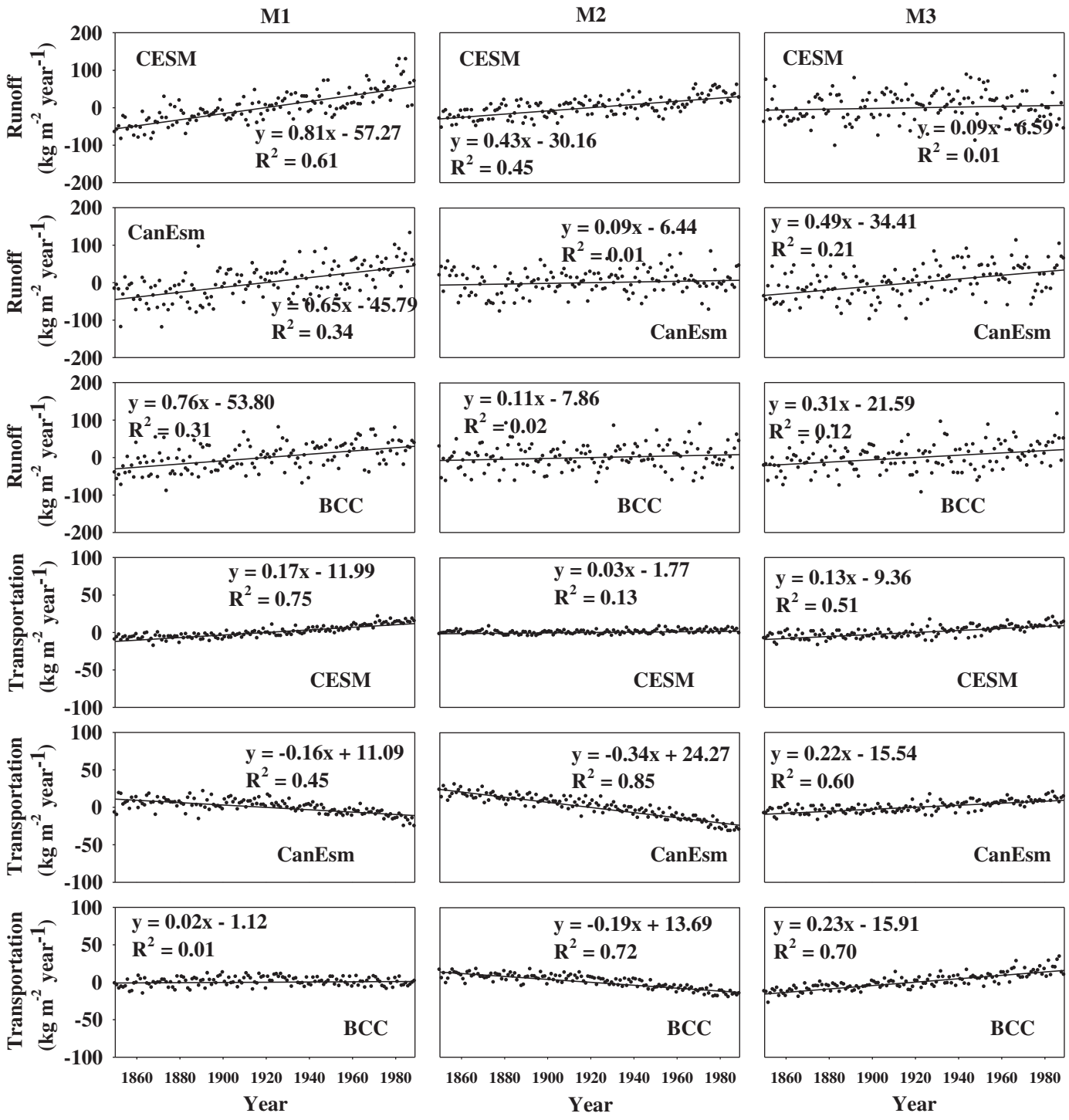

Fig. 8. Simulated annual changes in runoff and transpiration for the 140 years of the simulations of combined CO_2 physiological and radiative forcing (M1), physiological forcing (M2) and radiative forcing (M3). Lines are regressions and the symbols are averaged values of the Eastern Asia.

radiative and physiological forcing is close to the results reported by Boucher (changes of 3.5 vs. 0.5 °C in land surface temperature (the last three decades of the twenty-first century minus the last three decades of the twentieth century)) (Boucher et al., 2009). Fig. 3 shows the distribution of precipitation trends for the experiment M1, M2 and M3. Similar spatial patterns of precipitation changes in experiments of M1 and M3 appeared from the three models, especially in northern regions, where significant upward trends in precipitation are presented. The CO_2-radiative forcing results in coincident increases more than 0.4 mm/year^2 in Northern Asia, Northern America and Northern Europe in response to CO_2-radiative forcing (experiment M3). The Eastern Asia also exhibits a strong upward trend in averaged precipitation of 0.9 mm/year^2 from the 3 models (Table 2 and Figs. 2, 7). In contrast, in response to CO_2-physiological forcing, precipitation decreases in all of the three models over the global land (−0.02 mm/year^2 in CESM, −0.05 mm/year^2 in CanEsm and 0.00/mm/year^2 in BCC). This result is similar to Cao et al.

Table 2
Comparison of global precipitation, evapotranspiration, runoff and transpiration slopes (mm/year^2), correlation coefficients (R) and significant level (P) during 140 years.

		CESM			CANESM			BCC		
Experiments	Factors	Slope	R	P	Slope	R	P	Slope	R	P
M1	Precipitation	0.37	0.93	0	0.37	0.9	0	0.39	0.91	0
M2		−0.02	−0.2	0.02	−0.05	−0.31	0	0	0	0.97
M3		0.35	0.87	0	0.38	0.92	0	0.39	0.9	0
M1	Evapotranspiration	0.06	0.85	0	0.06	0.47	0	0.21	0.97	0
M2		−0.12	−0.97	0	−0.13	−0.82	0	−0.03	−0.58	0
M3		0.21	0.96	0	0.12	0.81	0	0.22	0.96	0
M1	Runoff	0.35	0.96	0	0.38	0.96	0	0.24	0.9	0
M2		0.13	0.88	0	0.08	0.69	0	0.04	0.41	0
M3		0.16	0.8	0	0.31	0.94	0	0.27	0.88	0
M1	Transpiration	0.08	0.92	0	−0.06	−0.79	0	−0.04	−0.81	0
M2		−0.01	−0.18	0.04	−0.09	−0.93	0	−0.1	−0.96	0
M3		0.1	0.89	0	0.02	0.54	0	0.03	0.69	0

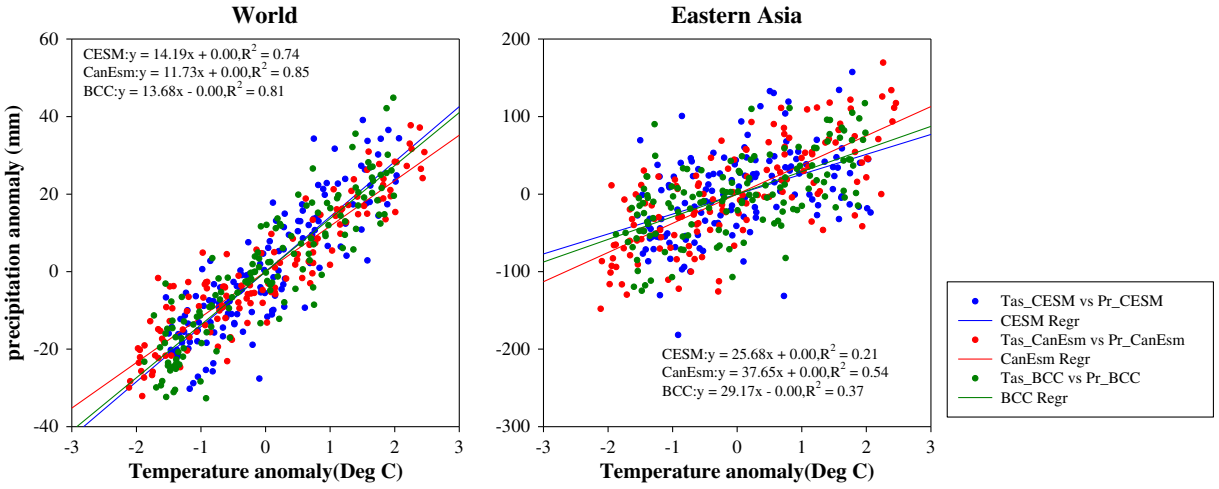

Fig. 9. Scatter plots of temperature anomaly and precipitation anomaly simulated by CESM, CanEsm, and BCC of experiment M3 over the world and Eastern Asia during the period of 1850–1989. Solid lines indicate linear relationships between temperature anomaly and precipitation anomaly.

(2012) who suggested that the physiological effect of increased atmospheric CO_2 on plant stomata reduces plant transpiration, which dries the boundary layer and decreases precipitation.

The general agreements about evapotranspiration among all of 3 models from experiment M1, M2 and M3 can be captured at the global and regional scales in Figs. 3 and 7. Responding to the CO_2-radiative forcing (experiment M3), there are significant increases in evapotranspiration in most land areas especially in northern latitudes e.g. Northern America, Northern Europe and Northern Asia. The upward global trends in evapotranspiration range from 0.12 mm/year^2 in CanEsm to 0.22 mm/year^2 in BCC at global scale. On average, about 74% of global land has shown significant increase from the experiment M3 of the 3 models. Similar spatial patterns of evapotranspiration changes also are seen in response to combined effect of CO_2-physiological forcing and CO_2-radiative forcing (experiment M1): the universally increased evapotranspiration in most northern latitudes and reduced evapotranspiration over low latitudes. In contrast, the reduction of evapotranspiration has been shown in response to CO_2-physiological effect (experiment M2). Over the global land, the downward trends in evapotranspiration associated with CO_2-physiological range from −0.82 mm/year^2 in CanEsm to −0.03 mm/year^2 in BCC.

At the global scale, there are coincident increases in runoff caused by the CO_2-radiative effect (experiment M3) from the three models. The measured areas with increasing runoff cover from 56% global land in CESM to 58% in CanEsm. The increase in runoff is due to the significant increase in precipitation (Leuzinger and K rner, 2010), which offsets more than the increase in evapotranspiration (0.37 mm/year^2 vs. 0.18 mm/year^2). Associated with CO_2-physiological forcing (experiment M2), the trend in runoff is relatively small from the 3 models, but the increase could be also expected similar to the most of studies (e.g.0.04 mm/day by Betts et al. (2007)) across the global land of about 0.07 mm/year^2. At the regional scale e.g. Eastern Asia, the effect of the radiative forcing alone also contributes to enhance the trend in runoff by 0.09–0.49 mm/year^2. In the same region, the CO_2-physiological forcing contributes to the upward trend in runoff by 0.01–0.43 mm/year^2. In Amazon Basin, reverse signs have been shown from the 3 models, in response to the CO_2-physiological forcing. Although precipitation has reduction of about −0.48 mm/year^2 (averaged by CESM, CanEsm and BCC), the increase in runoff is mainly as a result of diminished evapotranspiration from the world by about −0.55 mm/year^2 in response to CO_2-physiological forcing.

Trends of transpiration differently respond to effects of the increased CO_2 level from the 3 experiments depending on the simulated results by the 3 models. The effect of CO_2-phygeological forcing on transpiration results in reductions by −0.01, −0.09 and −0.1 mm/year^2 simulated by CESM, CanEsm and BCC over global land, respectively. These decreases mainly can be attributed to reductions in vegetation stomatal conductance because of atmospheric increased CO_2 concentration simulated (Kergoat et al., 2002). In contrast, increases in transpiration over global land respond to the effect of CO_2-radiative forcing by 0.1,

Fig. 10. Spatial distribution of correlation coefficients (R) between evapotranspiration and soil moisture simulated by CESM, CanEsm and BCC in response to combined CO_2-radiative and physiological forcing (experiment M1) ((a)–(c)), CO_2-physiological forcing (experiment M2) ((d)–(f)), CO_2-radiative forcing (experiment M3) ((g)–(i)), respectively, unitless.

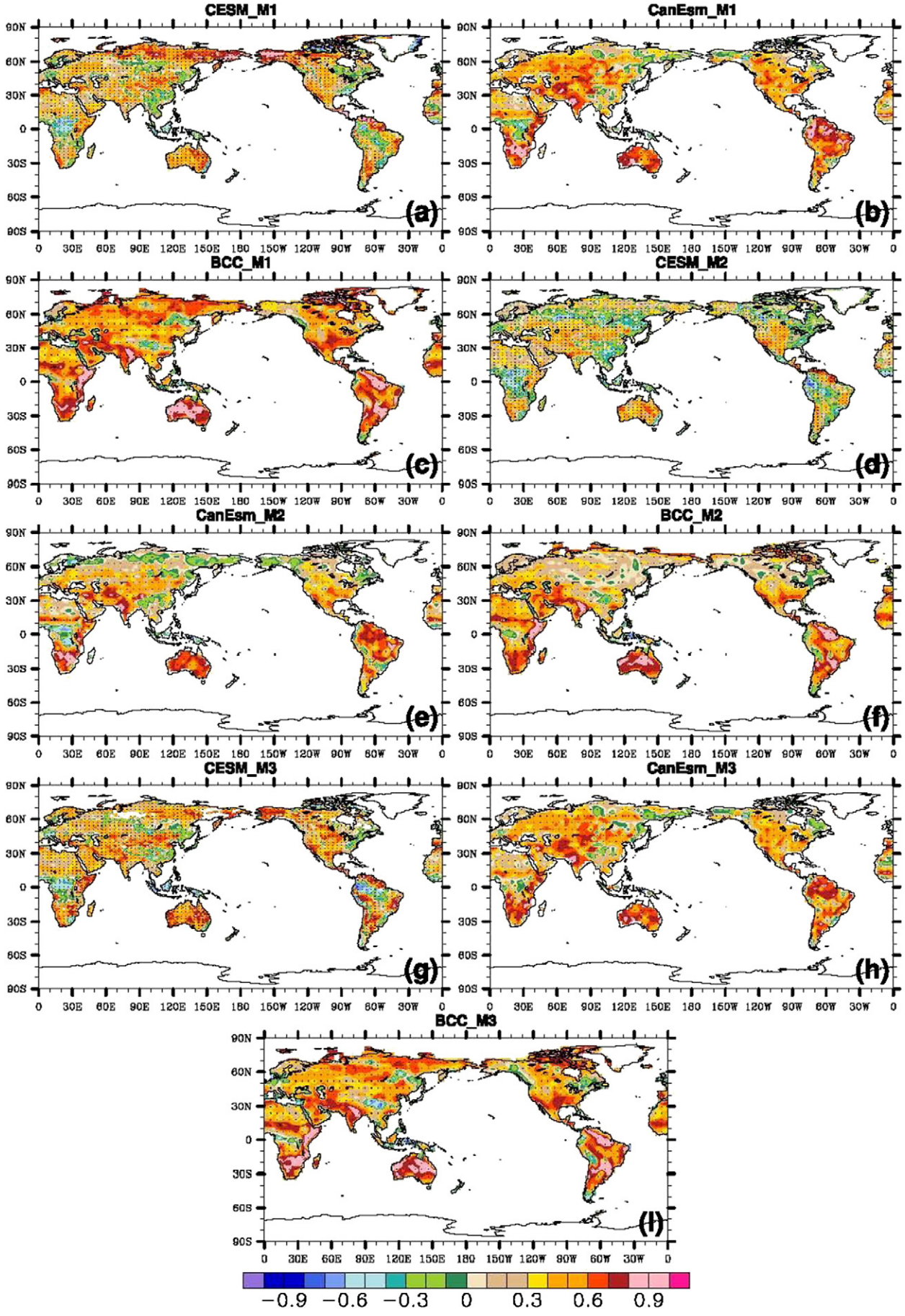
CESM_M1
CanEsm_M1
BCC_M1
CESM_M2
CanEsm_M2
BCC_M2
CESM_M3
CanEsm_M3
BCC_M3
(a)
(b)
(c)
(d)
(e)
(f)
(g)
(h)
(i)
90N
60N
30N
0
30S
60S
90S
0 30E 60E 90E 120E 150E 180 150W 120W 90W 60W 30W 0
−0.9 −0.6 −0.3 0 0.3 0.6 0.9

0.02 and 0.03 mm/year^2 simulated by the 3 models. The upward trend in transpiration is also shown from experiment M1 by CESM in response to combined effect of CO_2-physiological and CO_2-radiative forcing of 0.08 mm/year^2. In contrast, decreases of −0.06 and −0.04 mm/year^2 are presented from the same experiment by CanEsm and BCC. These differences in the stomatal mechanism and changes of leaf area index and vegetation distribution among the 3 models could lead to the differences in response to combined physiological and greenhouse effect.

From a global perspective, it is also worth noting that the soil moisture responds to CO_2-physiological forcing and CO_2-radiative forcing. All models show upward trends of global soil moisture during 140 years from the experiment M3 involving increasing CO_2 (0.008 kg/m^2/year in CESM to 0.38 kg/m^2/year in CanEsm). About 25% in CESM to 34% in BCC of the land surface shows the significant increases in soil moisture caused by CO_2-radiative forcing. Regardless of a general increase, in response to this forcing, regionally heterogeneous trends in soil moisture are easily depicted. The largest increases are located in northern high latitudes (e.g. Northern Asia, Eastern Asia and Northern Europe), while the significant reductions are seen in the low latitudes in the 3 models. Similar spatial patterns of the trend in soil moisture also are seen caused by the combined effect of CO_2-physiological and CO_2-radiative forcing. Associated with CO_2-physiological effect, averaged increases in soil moisture of the global land have ranged from 0.02 kg/m^2/year in CanEsm to 0.10 kg/m^2/year in BCC. Averaged over global land, about 24–32% land surface has significant upward trends in soil moisture in experiment M2. The magnitude of changes in soil moisture caused by CO_2-physiological forcing is usually less than CO_2-radiative forcing.

In all cases, the 3 models show greater contribution of CO_2-radiative forcing to the changes in hydrological variables than CO_2-physiological forcing. For example, on the 3 model averages, the changes in precipitation affected by CO_2-physiological forcing are only 6% changes caused by CO_2-radiative forcing. It is expected that the contribution of the same forcing has also a much smaller contribution to the changes of soil moisture compared with CO_2-radiative forcing. This is probably because of the greenhouse effect on changes in land hydrological cycle caused by CO_2-radiative forcing sufficiently enough to outweigh the mitigating effects of plant physiology e.g. CO_2-induced stomatal closure on the land water cycle (Bounoua et al., 1999; Levis et al., 2000).

4. Discussion

Few studies from multi-model experiments examined quantitative contribution induced by interactive effects caused by CO_2 physiological and radiative forcing on land water cycle associated with the increasing CO_2 concentration in atmosphere. At the 5% level using the student *t*-test, it is not significant that an increase in atmospheric CO_2 concentrations has interactive effects of physiological and radiative forcing on precipitation, evapotranspiration and runoff over global and regional scales simulated by CESM, CanEsm and BCC, respectively. Based on this conclusion, it can be deduced that contribution of CO_2-physiological forcing and CO_2-radiative forcing to land water cycle can be directly compared. Increase in association with CO_2-radiative forcing accounts for 88% to 100% of the total changes caused by the effects of CO_2-radiative and physiological forcing simulated by the three models, while decrease of precipitation caused by CO_2-physiological forcing accounts for less than 12% of those total changes. Hence, the precipitation trend is predominantly determined by CO_2-radiative forcing but not CO_2-physiological forcing based on the simulated results. In the same experiment, the models allow the CO_2-radiative forcing to take up about 67% and 74% of averaged increases in evapotranspiration and runoff produced by the same combined forcing.

As mentioned above for the three model results during the 140 years, the carbon–climate coupled models exhibit that the contribution of CO_2-radiative forcing to precipitation is much larger than the CO_2-physiological forcing. The differences of trends in precipitation are shown, responding to CO_2-physiological forcing and CO_2-radiative forcing: trends with physiological effect ranging from −0.05 mm^2/year^2 in CanEsm to 0.00 mm^2/year^2 in BCC; increases due to CO_2-radiative forcing varying from 0.35 mm^2/year^2 in CESM to 0.39 mm^2/year^2 in BCC. This strongly increased precipitation with the radiative effect may be due to the significantly increased temperature (Andrews, 2009) in response to CO_2-radiative forcing. For example, warming per degree simulated by the 3 models could induce an increased precipitation response (e.g. 13.20 mm/°C over the world, 30.83 mm/°C cross Eastern Asia in Fig. 9). Adler et al. (2008) suggested a longer observing time period of 1979–2006 and determined a precipitation response to warming (about +2.3% per degree) similar to simulated results in this analysis, neglecting the direct effect of forcing agents on precipitation. Nevertheless, compared with previous findings (Cao et al., 2009, 2010), our results consistently point to important implications of significant global warming caused by CO_2-radiative forcing for changes in precipitation. In response to 1% increasing CO_2 per year to quadrupling, precipitation here caused only by CO_2-physiological effects has slightly averaged decrease of 3 models. Ultimately, how CO_2 physiological forcing influences precipitation has also been investigated and the increase or no change has been suggested by the most previous studies similar to the result of this analysis (Cao et al., 2010). Andrews et al. (2011) reported that significant decreases of global precipitation over most land-regions attribute to main reductions to convective rainfall, involving reductions in near surface relative humidity, suppression of boundary-layer clouds (de Arellano et al., 2012) and latent heat flux (Ranjith, 2011) produced by CO_2 physiological forcing. Hence, we conclude that the effect of CO_2-physiological forcing on the precipitation should also not be neglected over the global land.

The simulated results by the 3 fully coupled models exhibit quite different responses of evapotranspiration to CO_2-physiological (experiment M2) and CO_2-radiative forcing (experiment M3). Averaged over the global land, there are increases in evapotranspiration caused by CO_2-raditive forcing depending on the 3 models. Jung et al. (2010) reported the recent decreases in the global land evapotranspiration due to the limited soil moisture supply. Understanding the way of the changes in evapotranspiration influenced by soil moisture would be useful in partitioning the surface water budget by evaporate water over the global land. It influences changes in the evapotranspiration at least in two main ways: directly dominating soil evaporation and affecting plant physiology and eventually leading to changes in transpiration. Thus, it is important to point out that the evapotranspiration is strongly reflected by the soil moisture in terms of magnitude and spatial pattern. Indeed, there is a fairly good agreement across the three models that increased evapotranspiration associates with the elevated soil moisture depending on experiment M3 at the global scale (e.g. 0.18 mm/year^2 vs. 0.18 kg/m^2/year over the world). A somewhat increased soil moisture thus mainly drives an increase of evapotranspiration (Siqueira et al., 2009; Seneviratne et al., 2010; Lawrence et al., 2012). From the view of the spatial pattern, using comprehensive fully coupled carbon–climate model, significant correlation coefficients between the evapotranspiration and soil moisture are shown in most regions (Fig. 10), especially in semi-arid and arid regions at 5% significant level. Responding to CO_2-radiative forcing presented here using the three models, the canopy transpiration increases only account for 14–48% of evapotranspiration. Cao et al. (2009) found that the strong increases in evapotranspiration are mainly dominated by the increases in soil evaporation from the global scale. However, the declines of evapotranspiration have been shown by the three models from −0.13 to −0.03 mm/year^2 in the response to physiological effect of increasing CO_2. The fractions of the reductions in transpiration account for 0.08–3.33 of the decreases in the global evapotranspiration. Hence, a source of uncertainty about the changes in components of the evapotranspiration can be attributed to the CO_2-physiological forcing in the process of canopy suppression of stomatal conductance versus increased LAI because of increasing atmospheric CO_2 (Cao et al., 2009; Barton et al., 2012). For example, in response to CO_2-physiological forcing, decreased canopy transpiration

plays an important role in changes in evapotranspiration obtained from CanEsm and BCC (e.g. −0.09 vs. −0.13 mm/year^2 in CanEsm). This result agrees with the conclusion reported by Cao et al. (2010) and shows that the transpiration is very sensitive to CO_2-induced stomatal closure with increase in atmospheric CO_2. But this is in sharp contrast to the simulated result from the low contribution of canopy transpiration to the evapotranspiration by CESM (−0.01 vs. −0.12 mm/year^2). These differences in the contribution of canopy transpiration to the evapotranspiration among the different models indicate that further studies based on effect of increasing CO_2 on stomatal conductance versus vegetation structure are needed to quantify the role that canopy transpiration plays in changes in evapotranspiration and global hydrological cycles.

Given these premises as mentioned above, a source of uncertainty could also be contributed to CO_2-physiological forcing similar to evapotranspiration. The runoff is mainly characterized as the difference of precipitation and evapotranspiration. Increases in runoff have been reported in previous studies due to the CO_2-physiological and CO_2-radiative influences (Gedney et al., 2006; Cao et al., 2010). In response to CO_2-physiological forcing, it is even less clear how the stomatal conductance and structural changes in vegetation (e.g. increased LAI) compete with each other associated with increased CO_2 in the atmosphere. It is well known that increases in runoff had been suggested by Gedney et al. (2006) and Betts et al. (2007) similar to this analysis, while Piao et al. (2007) had offered reduction in runoff in response to CO_2-physiological forcing due to increased LAI. Among models, significantly simulated increased runoff could be mainly contributed to the decreases in transpiration from CanEsm and BCC (e.g. 0.08 vs. −0.09 mm/year^2 in CanEsm) because of reductions in stomatal conductance (Field et al., 1995) caused by rising atmospheric CO_2 in experiment M2. In CESM, decrease in transpiration only accounts for 8% of the increase in runoff. These differences can be also found from the previous studies. Hence, there is still a large uncertainty on whether or not CO_2-physiological forcing attributes decreases in stomatal conductance to increasing runoff. Two models (e.g. CanEsm and BCC) attribute increasing runoff to CO_2-induced suppression of transpiration, while one model (CESM) shows that CO_2-induced suppression of transpiration cannot explain the increases in runoff. Therefore, the next step should be highly strengthened to study effects of CO_2-physiological forcing on the magnitude and sign of biophysical processes (e.g. suppression of stomatal conductance and structural changes in vegetation) and the hydrological cycle as mentioned above.

5. Summary

We have analysed whether or not interactive effects of CO_2-physiological forcing and CO_2-radiative forcing on the hydrological variables can be examined associated with increasing CO_2 in the atmosphere. There are no signs that the changes in precipitation, evapotranspiration and runoff respond to these interactive effects. The response of in precipitation and evapotranspiration to the CO_2-physiological effect is shown to be entirely different to the response to the greenhouse effect. In most land regions, there are statistically significant upward trends in precipitation and evapotranspiration (about 0.37 and 0.18 mm/year^2) in response to radiative effect due to the warming and increased soil moisture, respectively. If CO_2-physiological effect is only accounted for, there are downward trends in precipitation and evapotranspiration (about −0.02 and −0.09 mm/year^2). The increases in runoff are consistently indicated in all experiments derived from all models. These increases in response to CO_2-radiative forcing could be contributed to the increases in precipitation outweighing the increases in evapotranspiration. Generally, from the pattern of spatial distribution, hydrological variables including precipitation, evapotranspiration and runoff have much larger response to the CO_2-physiological forcing than to the CO_2-radiative forcing. With the physiological effect, increases in the runoff could be mainly contributed to the reduction in transpiration simulated by CanEsm and BCC (the transpiration trends of −0.09 mm/year^2 vs. the runoff trends of 0.08 mm/year^2 in CanEsm). In the same experiment, this decrease could not explain the increase in runoff by CESM (−0.01vs. 0.13 mm/year2). The CO_2 physiological forcing is a source of the many uncertainties when plant physiology is considered into the land hydrological cycle. The change in stomatal conductance versus change in vegetation structure (e.g. increased LAI) caused by the CO_2-physiological forcing is quite subject to debate among the different earth system models. In a more integrated way, the next step would be focused on estimating and comparing of the simulated results by more different earth system models in response to CO_2-physiological forcing caused by increased CO_2 levels in atmosphere.

Acknowledgements

This study was supported by the Knowledge Innovation Program of the Chinese Academy of Sciences (KZCX2-EW-QN208 and 7-122158), the CAS Strategic Priority Research Program (grant no. XDA05110103), the National Basic Research Program of China (grant no. 2010CB 950500), and the project of National Natural Science Foundation of China (grant no. 41275082 and 41305070).

References

Adler, R.F., et al., 2008. Relationships between global precipitation and surface temperature on interannual and longer timescales (1979–2006). J. Geophys. Res. 113 (D22104). http://dx.doi.org/10.1029/2008JD010536.
Andrews, T., 2009. Forcing and response in simulated 20th and 21st century surface energy and precipitation trends. J. Geophys. Res. 114 (D17). http://dx.doi.org/10.1029/2009JD011749.
Andrews, T., Doutriaux-Boucher, M., Boucher, O., Forster, P., 2011. A regional and global analysis of carbon dioxide physiological forcing and its impact on climate. Clim. Dyn. 36 (3–4), 783–792.
Bala, G., Caldeira, K., Nemani, R., 2010. Fast versus slow response in climate change: implications for the global hydrological cycle. Clim. Dyn. 35 (2–3), 423–434.
Bala, G., et al., 2011. Albedo enhancement of marine clouds to counteract global warming: impacts on the hydrological cycle. Clim. Dyn. 37 (5–6), 915–931.
Barton, C.V.M., et al., 2012. Effects of elevated atmospheric CO_2 on instantaneous transpiration efficiency at leaf and canopy scales in Eucalyptus saligna. Glob. Chang. Biol. 18 (2), 585–595.
Betts, R.A., et al., 2007. Projected increase in continental runoff due to plant responses to increasing carbon dioxide. Nature 448 (7157), 1037–1041.
Bonan, G.B., Levis, S., 2010. Quantifying carbon–nitrogen feedbacks in the Community Land Model (CLM4). Geophys. Res. Lett. 37 (7). http://dx.doi.org/10.1029/2010GL042430.
Bonan, G.B., Hartman, M.D., Parton, W.J., Wieder, W.R., 2012. Evaluating litter decomposition in earth system models with long-term litterbag experiments: an example using the Community Land Model version 4 (CLM4). Glob. Chang. Biol. http://dx.doi.org/10.1111/gcb.12031.
Boucher, O., Jones, A., Betts, R., 2009. Climate response to the physiological impact of carbon dioxide on plants in the Met Office Unified Model HadCM3. Clim. Dyn. 32 (2–3), 237–249.
Bounoua, et al., 1999. Interactions between vegetation and climate: radiative and physiological effects of doubled atmospheric CO_2. J. Clim. 12, 309–324.
Cao, L., Bala, G., Caldeira, K., Nemani, R., Ban-Weiss, G., 2009. Climate response to physiological forcing of carbon dioxide simulated by the coupled Community Atmosphere Model (CAM3.1) and Community Land Model (CLM3.0). Geophys. Res. Lett. 36 (10), L10402.
Cao, L., Bala, G., Caldeira, K., Nemani, R., Ban-Weiss, G., 2010. Importance of carbon dioxide physiological forcing to future climate change. Proc. Natl. Acad. Sci. 107 (21), 9513–9518.
Cao, L., Bala, G., Caldeira, K., 2012. Climate response to changes in atmospheric carbon dioxide and solar irradiance on the time scale of days to weeks. Environ. Res. Lett. 7 (3), 034015.
Christian, et al., 2010. The global carbon cycle in the Canadian Earth system model (CanESM1): preindustrial control simulation. J. Geophys. Res. 115 (G3). http://dx.doi.org/10.1029/2008JG000920.
Cramer, W., et al., 2001. Global response of terrestrial ecosystem structure and function to CO2 and climate change: results from six dynamic global vegetation models. Glob. Chang. Biol. 7 (4), 357–373.
Dan, L., Ji, J., Li, Y., 2005. Climatic and biological simulations in a two-way coupled atmosphere–biosphere model (CABM). Glob. Planet. Chang. 47 (2–4), 153–169.
de Arellano, J.V., van Heerwaarden, C.C., Lelieveld, J., 2012. Modelled suppression of clouds by boundary-layer plants in a CO_2-rich atmosphere. 5 (10), 701–704.
Doutriaux-Boucher, M., Webb, M.J., Gregory, J.M., Boucher, O., 2009. Carbon dioxide induced stomatal closure increases radiative forcing via a rapid reduction in low cloud. Geophys. Res. Lett. 36 (2). http://dx.doi.org/10.1029/2008GL036273.
Field, C.B., Jackson, R.B., Mooney, H.A., 1995. Stomatal responses to increased CO2: implications from the plant to the global scale. Plant Cell Environ. 18 (10), 1214–1225.
Gedney, N., et al., 2006. Detection of a direct carbon dioxide effect in continental river runoff records. Nature 439 (7078), 835–838.

Gerten, D., Schaphoff, S., Lucht, W., 2007. Potential future changes in water limitations of the terrestrial biosphere. Clim. Chang. 80 (3–4), 277–299.
Gillett, N.P., Arora, V.K., Zickfeld, K., Marshall, S.J., Merryfield, W.J., 2011. Ongoing climate change following a complete cessation of carbon dioxide emissions. Nature 4 (2), 83–87.
Giorgi, F., Francisco, R., 2000. Evaluating uncertainties in the prediction of regional climate change. Geophys. Res. Lett. 27 (9), 1295–1298.
Ji, J.J., 1995. A climate–vegetation interaction model: simulating physical and biological processes at the surface. J. Biogeogr. 22 (2–3), 445–451.
Jung, M., et al., 2010. Recent decline in the global land evapotranspiration trend due to limited moisture supply. Nature 467 (7318), 951–954.
Kergoat, L., et al., 2002. Impact of doubled CO2 on global-scale leaf area index and evapotranspiration: conflicting stomatal conductance and LAI responses. J. Geophys. Res. Atmos. 107 (D24) (ACL 30-1-ACL 30-16).
Lawrence, D.M., et al., 2011. Parameterization improvements and functional and structural advances in Version 4 of the Community Land Model. J. Adv. Model. Earth Syst. 3, 1. http://dx.doi.org/10.1029/2011MS000045.
Lawrence, et al., 2012. Simulating the biogeochemical and biogeophysical impacts of transient land cover change and wood harvest in the Community Climate System Model (CCSM4) from 1850 to 2100. J. Clim. 25 (9), 25.
Leuning, R., 1995. A critical appraisal of a combined stomatal-photosynthesis model for C3 plants. Plant Cell Environ. 18 (4), 339–355.
Leuzinger, S., K rner, C., 2010. Rainfall distribution is the main driver of runoff under future CO_2-concentration in a temperate deciduous forest. Glob. Chang. Biol. 16 (1), 246–254.
Levis, S., Foley, J.A., Pollard, D., 2000. Large-scale vegetation feedbacks on a doubled CO2 climate. J. Clim. 13 (7), 1313–1325.
Peng, J., et al., 2013. Effects of increased CO_2 on land water balance from 1850 to 1989. Theor. Appl. Climatol. http://dx.doi.org/10.1007/s00704-012-0673-3.
Piao, S., et al., 2007. Changes in climate and land use have a larger direct impact than rising CO2 on global river runoff trends. Proc. Natl. Acad. Sci. 104 (39), 15242–15247.
Ranjith, G.A.G.B., 2011. Sensitivity of terrestrial water and energy budgets to CO_2-physiological forcing: an investigation using an offline land model. Environ. Res. Lett. 6 (4), 044013.
Risnen, J., 2002. CO_2-induced changes in interannual temperature and precipitation variability in 19 CMIP2 experiments. J. Clim. 15 (17), 2395–2411.
Seneviratne, S.I., et al., 2010. Investigating soil moisture–climate interactions in a changing climate: a review. Earth Sci. Rev. 99 (3–4), 125–161.
Siqueira, M., Katul, G., Porporato, A., 2009. Soil moisture feedbacks on convection triggers: the role of soil–plant hydrodynamics. J. Hydrometeorol. 10 (1), 96–112.
Solomon, S., Plattner, G., Knutti, R., Friedlingstein, P., 2009. Irreversible climate change due to carbon dioxide emissions. Proc. Natl. Acad. Sci. 106 (6), 1704–1709.
Sugi, M., Yoshimura, J., 2004. A mechanism of tropical precipitation change due to CO_2 increase. J. Clim. 17 (1), 238–243.
Taylor, K.E., Stouffer, R.J., Meehl, G.A., et al., 2012. An overview of CMIP5 and the experiment design. Bull. Amer. Meteor. Soc. 93 (4), 485–498.
Tenhunen, J., et al., 2009. Influences of changing land use and CO2 concentration on ecosystem and landscape level carbon and water balances in mountainous terrain of the Stubai Valley, Austria. Glob. Planet. Chang. 67 (1–2), 29–43.
Zhang, L., Dong, M., Wu, T., 2011. Changes in precipitation extremes over Eastern China simulated by the Beijing Climate Center? Climate System Model (BCC_CSM1.0). Clim. Res. 50 (2–3), 227–245.
Zhu, Q., et al., 2012. Effects of future climate change, CO2 enrichment, and vegetation structure variation on hydrological processes in China. Glob. Planet. Chang. 80–81, 123–135.